Thermal Runaway Detection in Li ion Cells

Author: Richard Johnson

The University of Sheffield, Department of Chemical and Biological Engineering

Student Number: 140127968

Email: RCJohnson2@sheffield.ac.uk

Abstract

Although efforts have been made to improve the safety of Li ion cells via the introduction of safety mechanisms (CIDs, PTCS), these devices are incapable of detecting the onset of thermal runaway and do not always provide effective protection from energetic failure. It is therefore important that we develop techniques to detect impending thermal runaway, but so far very little progress has been made in this field. It is argued through the use of literature examples that the data obtained through non-invasive monitoring of cell temperature, voltage, current, and resistance could be used to identify early warning signs of thermal runaway. The idea of implementing a slight separator modification to allow early detection of lithium dendrite shorts is explained and discussed, and the problems associated with scaling-up the described techniques are briefly explored.

1. Introduction

Li ion cells are one of the most frequently implemented energy storage devices in the world, and are the primary choice of power source for consumer electronics, electric vehicles, and powertools [1]. The commercial success of Li ion is attributed mainly to the impressive cycle life and high energy density that the family of cell chemistries presents [2]. However, this high energy density impacts the safety of Li ion cell operation; cells are able to generate their own heat through a series of exothermic decomposition reactions that begin when the cell reaches 70-80^{o}C [3], and if the rate of heat generation exceeds the rate of heat loss to the surroundings, the cell will continue to rise in temperature and may ultimately vent ignited gases (these are generated as a product of decomposition). This energetic failure mode is usually referred to as thermal runaway (TR).

High profile examples of Li ion TR include the recall of 4.1 million dell laptops in 2006 due to a series of battery pack fires, and several Boeing 787 Dreamliner electrical system faults that resulted from the energetic failure of the defective Li ion packs [4].

Although systems are usually put in place to protect cells (Charge interrupt devices, Positive temperature coefficient switches, overcharge and over-discharge protection, shutdown separators *etc.*) they are not always effective, and so energetic failure often occurs regardless of precautions and without any warning. There are no well-known or widely applied techniques for predicting an impending

thermal runaway, but development and application of such techniques may allow enough time for the failing cell to be removed from a pack (thus preventing propagation of TR to neighbouring cells), and may even allow us to predict failure long before self-heating begins.

The following review aims to explain the fundamentals of TR, and provide examples of research that supports the possibility for development of an early warning system.

2. Theory

2.1 Li ion Heat Balance and The Thermal Runaway Process

During cell operation, heat is continuously generated by chemical and physical processes, and dissipated through convective and radiative processes. A cell enters TR when the rate of internal heat generation exceeds the rate of heat dissipation through convection and radiation. In a Li ion cell, the rate of heat loss increases linearly with T, but the rate of heat generation increases exponentially with T (mainly because the number of exothermic decomposition processes occurring, and their respective rates, increase with T). This means that a critical temperature is reached above which the cell cannot fully dissipate the heat it generates, and a positive feedback process begins in which $\frac{dT}{dt}$ increases as T increases. This temperature is often termed the 'temperature of no return', T_{NR} [3], and its value depends on the quality of the cells' cooling system (fig. 1).

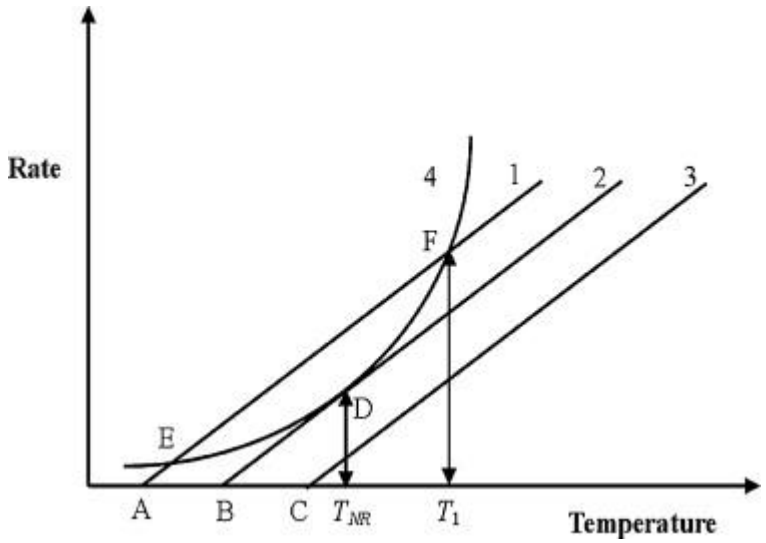

Fig. 1 - Shows the rate of heat loss as a function of T for cells A, B, and C together with an exponential function representing heat generation as a function of T. Point D marks the T at which heat generation rate is equal to heat dissipation rate, and extrapolation to the x-axis yields T_{NR}. Cell cooling capabilities decrease from A – C [5].

The equation representing cell heat balance is widely accepted to take the following form:

$$\frac{\partial(\rho C_p T)}{\partial t} = -\nabla(k\nabla T) + Q_{ab-chem} + Q_{joul} + Q_S + Q_P + Q_{ex} \ldots$$

Where k is thermal conductivity, T is temperature, Q_s is heat by entropy change, Q_p is overpotential heat, and Q_{ex} is heat exchange between the system and its surroundings via radiation and convection. $Q_{ab\text{-}chem}$ represents the total heat generation associated with all internal reactions, and mainly consists of exothermic SEI and electrode decomposition processes [3]. The rate of heat released by any given reaction is calculated by:

$$\frac{\partial H}{\partial t} = \Delta H M^n A e^{-\frac{E_a}{RT}}$$

Where ΔH is enthalpy change of reaction, E_a is activation energy, M is reactant mass, n is reaction order, and A is the pre-exponential factor. The sum of $\frac{\partial H}{\partial t}$ for all cell reactions represents the largest portion of total internal heat generation during TR.

Q_{joul} represents the heat generated via joule heating, and may be calculated as:

$$Q_{joul} = \sum_j \left|\varphi_j \cdot i_j\right|$$

Where φ_j represents potential across phase j (where phase j may be the anode, cathode, electrolyte, separator *etc.*), and i_j represents current density in phase j. Joule heating often results from the formation of shorts with the cell, and from the presence of high impedance welds and connections. Although it is usually not the primary source of internal heat generation at high temperatures, it often provides the heat necessary to raise the cell to T_{NR}.

At 70-80ºC thermal runaway begins as exothermic anodic reactions occur [6]. At 120-130ºC, the SEI begins to decompose into the electrolyte at a significant rate. This process evolves heat, which raises the temperature and the rate of SEI decomposition, which further increases the rate of heat generation. This positive feedback effect continues up until the point that the cell fails, which may involve venting and combustion of evolved gases [3]. As cell temperature increases the activation barriers for other chemical and physical processes are overcome, and these processes may also contribute to thermal runaway (table 1). The 70-80ºC internal temperature required for thermal runaway to occur may be reached due to the joule heating that results from internal shorting and/or poor cell cooling, amongst other things [7].

Temp (ºC)	Reaction	Energy (J/g)
120-130	SEI Decomposition	200 → 350
130-170	Separator Melts	-190 → -90
200	Solvent + Electrolyte	300
240-250	LiC_6 + Binder	300-500
240-250	LiC_6 + Electrolyte	1000-1500
200-230	Cathode Decomposition	1000

Table 1 – chemical and physical reactions that become significant between 120 – 230ºC are shown. Results were obtained via differential scanning calorimetry, and the increased potential for heat evolution with increased temperature can be clearly seen.

2.2 Cell Abuse

The following section describes the various mechanisms via which TR may be initiated**.**

2.2.1 Thermal abuse

The process by which a cell is brought to the temperature required to initiate thermal runaway via exposure to a high external temperature or through being situated in a heavily insulated area (so rate of loss of internally generated heat is greatly reduced).

2.2.2 Over-discharge

The process by which Li ion cell potential is brought below the range of safe values. Over-discharge causes the potential at the copper current collector to increase to the point that the metal becomes unstable and is oxidised, resulting in dissolution of ions into the electrolyte solution. On charging, these ions become unstable and are precipitated as metallic copper on the anode. Lithium can no longer be intercalated into the anode pores, and so it is plated upon the copper layer. This results in the formation of lithium dendrite that can grow to form a short, which in turn results in joule heating (due to current flow and voltage drop across the resistive short) that raises the internal cell temperature and initiates TR. If internal shorts are accidentally introduced to a cell during manufacturing, over-discharge may occur in storage.

2.2.3 Overcharge

The process by which the Li ion cell potential is brought above the range of safe values. Over charge can cause lithium plating at the anode to occur more readily than intercalation, which results in the formation of lithium dendrite shorts, leading to joule heating and TR. The plated lithium can also react exothermically with the electrolyte, and the cathode may become unstable as a result of excess lithium

removal, causing an exothermic decomposition process to occur. Both of these reactions result in a heat release that increases cell internal temperature and may lead to TR.

2.2.4 External Shorting

External shorting may cause joule heating at localised areas of high impedance within the cell (e.g. weld points and electrode surfaces. If the heat generation rate is sufficient, then the cell may enter TR. This failure mechanism is a higher risk to larger cells which contain larger quantities of electrode material and have poorer heat transfer properties as a result of their size.

2.2.5 Mechanical Abuse

Physical mishandling of a cell. Mechanical abuse may cause internal cell damage that immediately, or eventually leads to short formation. In the former case, the abuse causes electrically conductive components of the cell to make contact and internally short the cell. This results in localised joule heating that rapidly raises the cell temperature to the TR threshold. In the latter case, lithium plating occurs at a site of minor mechanical damage, and the resulting dendrite formation leads to shorting, joule heating, and ultimately TR – this is far more problematic than the former situation, as a cell will function correctly for some duration (and so problems will not be detected during initial testing), then enter TR during field operation. Mechanical defects may also be introduced during manufacturing; electrode misalignment, electrode damage, short-forming contaminants, and weld spatter defects are all potential causes of immediate or latent cell failure [7].

2.3 Current TR prevention mechanisms and Their Limitations

Thermal management is usually limited to the installation of Positive temperature coefficient (PTC) switches, which are commonly integrated into battery management systems, and consist of a thin polymer layer that becomes highly resistive at high temperatures. This prevents the flow of current through the cell and reduces joule heating effects. Though somewhat effective in preventing runaway, such devices prevent cells from operating at a high current (as high current results in significant joule heating and consequently high PTC switch resistance), and may be unsafe in systems with many cells connected in parallel [8]. Most importantly, such devices become ineffective at temperatures exceeding 150^{o}C, and therefore provide no protection or warning when thermal runaway in entered rapidly.

A charge interrupt device (CID) may be used to irreversibly disconnect a cell from a pack, and is set to activate when the internal pressure of the cell reaches a predefined value determined by the CID design. The pressure build up occurs as a result of gas evolution from the electrode decomposition process, which occurs during TR [7]. It is not possible to operate a cell that contains a CID at high currents, and it is likely that in large packs CIDs may activate in cascade; the shutdown of one cell may cause a sudden overcurrent in another, forcing it into TR if its own CID does not activate promptly enough [8].

It has therefore become necessary to develop other techniques with which to monitor and interpret cell parameters that will not impact on their performance and may provide an earlier and more reliable warning of impending thermal runaway.

2.4 Boeing 787 Dreamliner Incidents

In January 2013, all American Boeing 787 Dreamliner passenger jets were grounded due to severe Li-ion battery faults that were responsible for a number of electrical failures and fires. NTSB investigators visited the facility in which the defective batteries were produced, and found the potential contamination with debris during the welding process, and misfolded cell windings to be a likely cause of the previous failures. The authors conclude that TR may have been initiated by short circuit formation within the cell, resulting from lithium dendrite formation on defects.

In further studies, engineers also found inconsistency in the resistance of riveted joints that connected separate cells to the conduction path; the resistance across the aluminium rivet–current collector joint of one cell was more than 1000 times greater than that of the others. This high resistance resulted in localised joule heating and exposed the cell to temperatures up to 157^{o}C, causing the separator to melt. The report notes that the temperature in the defective systems was recorded on two-cell bus bars, so these much higher localised cell temperatures were not observed, and states that cell level temperature monitoring and trend analysis may provide an early warning of TR that the flight crew and maintenance staff may be able to act upon [4]. The authors suggest that the recognition of TR early warning signals may allow such a problem to be solved.

3 Literature Review

3.1 Early Detection of Short Formation using Bifunctional Separators

Fouchard and Lechner (1992), categorise internal shorts as ‘hard’ and ‘soft’. A soft short is considered to be any high impedance short that results in slow self-discharge of a cell, whereas any low impedance shorts that may lead to sudden discharge and energetic failure are deemed hard shorts [9]. The authors note that formation of soft internal shorts is the most common first step in the Li ion failure process, and that any technique that can be used to detect internal shorts may be a useful indicator of impending hard short formation and TR.

Darcy and Keyser (2014) examined the effect of different types of shorts on the likelihood of TR [10]. Both anode-cathode collector and collector-collector shorts were seen to initiate TR, and anode-cathode collector shorts were not prevented by the inclusion of a shutdown separator. Cathode-anode collector contact resulted in a high impedance soft short that did not result in a TR event.

With the aim of detecting dendritic lithium growth before it caused shorting, Wu et al. (2014) produced a cell with a separator composed of a 50 nm layer of copper sandwiched between two 12 µm layers of

porous polymer [11]. This construction was given the name ‘bifunctional separator’ because it functioned as both a standard separator and as a voltage sensor; when a dendrite formation penetrates the separator it makes contact with the conductive metal layer and a voltage drop can be detected across the anode and metal.

The separator was constructed by magneto sputtering the 50 nm copper layer onto the 12 μm porous polymer substrate, then placing the second polymer layer onto the copper coating. The magneto sputtering process allowed deposition of the conducting layer without additional heat, thus preventing thermal degradation of the polymer substrate and maintaining its porous structure. The very low thickness of the conducting layer allowed the mechanical properties of the separator to be maintained, so integration of the new device into a full working cell presented no new construction challenges.

The group constructed a cell composed of two lithium metal electrodes and a standard separator, and measured potential between electrodes ($V_{Li\text{-}Li}$) as a function of time. It was seen that cell potential increased gradually from 200 mV to 500 mV due to the increased cell impedance resulting from SEI formation, then sharply decreased to near zero due to the formation of a dendrite short between electrodes (fig. 2).

The same process was repeated with a cell containing two lithium metal electrodes and a bifunctional separator. The observed behaviour was identical to that of the cell containing the standard separator for the first 3.5 h, after which a drop in potential between anode and separator from 3000 mV to 0 mV was observed. This was attributed to shorting between the anode and copper conductor through a lithium dendrite formation, and this was confirmed by observing the same process in a transparent pouch cell with optical microscope. A simultaneous drop in $V_{Li\text{-}Li}$ from 500 mV to 250 mV was also observed, and is attributed to the sudden decrease in total cell impedance resulting from the electronic short. The cell potential gradually recovered to 500 mV as a new SEI layer formed on the copper nanolayer.

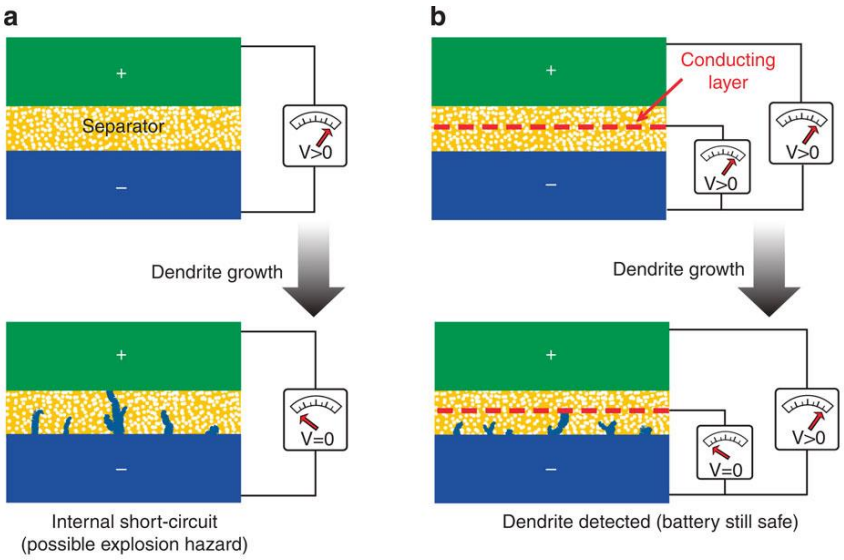

Fig 2 - (a) the short circuit induced voltage drop observed in a cell containing a standard separator (b) the voltage drop between anode and cathode, and anode and separator upon lithium dendrite shorting between anode and separator.

It was noted that by varying the thickness ratio between the two porous polymer layers, it was possible to vary the level of separator penetration upon which the voltage drop between the anode and copper layer occurred. This suggests that the amount of warning time for impending cell failure could be easily varied during separator construction. The same experiment was performed on a $LiCoO_2$/Li battery, and similar results were obtained.

The study was extended to show that the point of dendrite growth/penetration on the copper layer could be pinpointed with reasonable accuracy using a simple resistance monitoring technique (fig. 3). A single pinhole was made in the bifunctional separator to influence localised dendrite growth. After cycling, the resistance between opposite ends of the copper nanolayer ($R_1 + R_2$), and the resistances between each end of the copper nanolayer and the anode lead ($R_1 + R_{Junc}$, $R_2 + R_{Junc}$) were measured. Using these values, the fixed Li-Cu junction resistance R_{Junc} was calculated, and the ratio R_1/R_2 was determined. Using the relationship,

$$\frac{R_1}{R_2} = \frac{L_1}{L_2}$$

where L_1/L_2 may be used to determine the position of the dendritic growth, the group were able to confirm a very close agreement between the calculated and known positions of the pinholes; the percentage difference between these two values did not exceed 1.5 % over 10 samples.

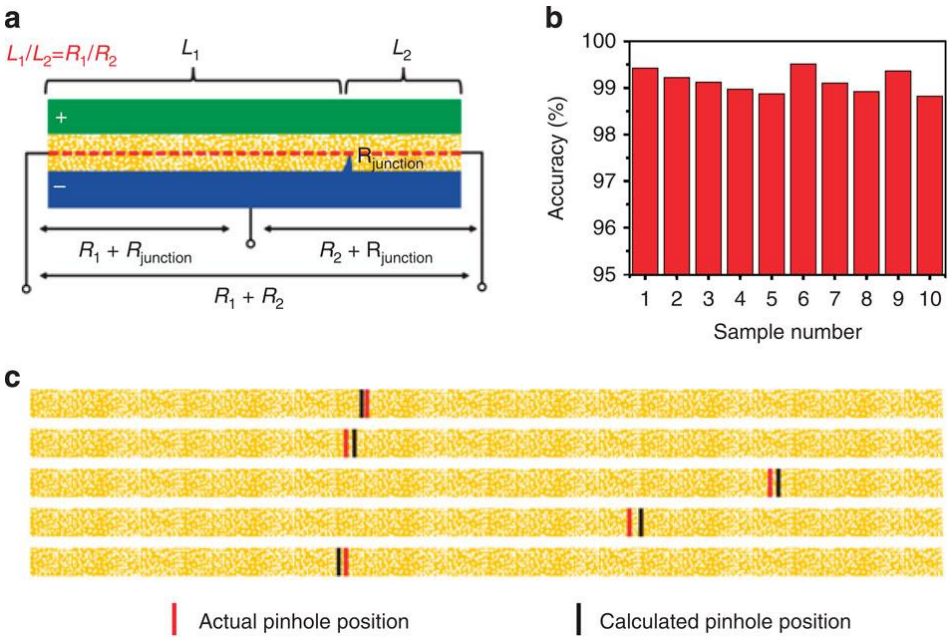

Fig 3 – (a) shows resistance pathways used to calculate L_1 and L_2, and the physical meaning of L_1 and L_2, (b) shows the percentage difference between the true position and calculated position of each pinhole, (c) shows actual and calculated pinhole positions in 5 of the test performed.

It is suggested that the added safety contributed by this technology should allow us to decrease the separator thickness without increasing risk of thermal runaway, and so energy density should not be decreased by addition of the bifunctional separator. It is noted that it may be challenging to include the separator in a cylindrical cell, but that the structure could be easily be integrated into a pouch cell. With consideration to the similarities in geometry between pouch and prismatic cells, it is likely that an attempt to include a bifunctional separator in the latter could also be successful.

Though not confirmed experimentally, it is suggested that the bifunctional separator should function with almost any Li-ion chemistry. No other methods for coating the porous polymer with copper are suggested, though particle coating, gel electrolyte coating, electrospinning of polymer fibres, and copolymer coating are all suggested as methods with which to add the second polymer layer.

The study has clearly yielded a promising and potentially diverse technique with which to safely detect the formation of hard shorts before they lead to thermal runaway. The diagnostic method may be effective in situations of electrical and mechanical abuse, but may not be effective in situations where cells enter TR as a result of thermal abuse. Studies into separator production, compatibility with other chemistries and geometries, and scale-up should be carried out before the technique is considered for commercial application, and the practicality of implementing the bifunctional separator device into commercial cells should be considered.

3.2 Predicting Mechanical and Electrical Abuse Triggered TR via Non-Invasive Measurement of Cell Parameters

Mikolajczac (2010) performed cycling tests on cells with known faults, and observed numerous artefacts in the charging/discharging profile that would not be expected of a healthy cell. All of these behaviours became observable many hours before the cell entered thermal runaway [12].

Lab produced coin cells were connected in parallel with commercial prismatic cells containing the same anode, cathode and separator material, and deliberate damage and faults were induced in the cells, such as contamination, separator damage, and regions of bare copper. The resulting parallel arrangement was noted to be electronically equivalent (in terms of external testing) to a larger prismatic cell with a localised fault. Thermocouples were attached to coin cell surfaces so that thermal runaway could be detected when it occurred.

Undamaged prismatic cells were cycled and the resulting charge/discharge profiles were used as a control that the charge/discharge profiles for the damaged coin cell system could be compared to. The parallel coin cell – prismatic cell systems were cycled until thermal runaway was entered.

Thermocouples detected a temperature increase associated with thermal runaway at an average of 20 h after cycling began. During the 20 h between cycling initiation and runaway, three unexpected cell behaviours were observed; elevated self- discharge rates, extended taper current times, and a divergence in charge vs. discharge capacity (more than would be expected due to general aging).

Commercial 18650 cells with known anode-cathode misalignments were cycled using a program intended to simulate real life Li-ion battery usage in a laptop. The program included extended rest after charging and discharging, secondary taper current charging step after a full charge rest period (to simulate the presence of a parallel cell that may provide current to a faulty cell), and partial charges and discharges. No cells entered thermal runaway during the course of the testing, and no cells exhibited elevated self-discharge rates. These observations are attributed to the absence of any durable internal shorts. Cells showed long taper current charging times during some cycles, and frequently exhibited sharp voltage and current changes during charging – both observations were attributed to the formation of temporary micro-shorts.

The authors conclude that the artefacts observed may be used to predict thermal runaway in Li-ion cells before such a state is entered. It is noted that further work must be performed to ensure that the technique is applicable to different cell shapes, sizes, chemistries, and scales (i.e. packs), and that similar behaviour is observed in cells that are subjected to real field conditions. A need to determine threshold values for the failure prediction parameters (e.g. self-discharge rate) is asserted, and it is suggested that obtaining and testing cells from imbalanced battery packs may accelerate the development of data sets that could provide a base from which threshold values could be developed.

Xiong (2012), used rule based and probabilistic methods to predict impending failure in A123 18650 cylindrical $LiFePO_4$ cells [13]. Preliminary experiments consisted of repeatedly over-discharging then recharging to 100%. All cells failed after 3 cycles, and two distinct failure signatures were observed; temperature increased rapidly and reached levels much higher than that expected of a healthy cell before entering thermal runaway, and voltage decreased significantly before the cell entered runaway. An algorithm was programmed which included the following rules:

$$\text{If } T_{cell} > T_{max} + \delta_T, \text{ issue warning}$$

$$\text{If } V_{i-k} - V_i > \beta_v, \text{ issue warning}$$

Where T_{cell} and V_i are the surface temperature and voltage of the cell at any given time, T_{max} is the maximum surface temperature reached by the cell during over-discharge, δ_T is the threshold above T_{max} which T_{cell} must exceed in order for a warning to be issued, V_{i-k} is the voltage at some time 'k' before V_i (used to eliminate noise effects), and β_v is the voltage difference threshold, above which a warning is triggered.

To develop the probabilistic part of the algorithm, numerous cells were over-discharged and cycled to failure, and the parameters T_B (maximum cell surface temperature observed in final discharge before failure) and T_F (surface temperature at failure) were extracted. Following this, the following equation was solved for each cell:

$$T_D = T_F - T_B$$

T_D, the temperature difference of failure, was seen to follow a normal distribution. The distribution of T_D was described mathematically by the probability density function f(x), and failure probability at any given time was estimated as:

$$P = \int_{-\infty}^{T_{cell}-T_B} f(x)dx$$

Where T_B equals the max temperature observed during the previous over-discharge, and was updated every cycle.

Cells were tested at 25ºC, 35ºC, and 45ºC, at charging rates 1C, 2C and 3C, and the algorithm was administered by an NI Compact RIO system. The rule based section of the algorithm accurately detected impending runaway under all testing conditions, and runaway was usually detected by temperature increase above threshold (fig. 4) (although detection by voltage decrease did sometimes occur first). Thermal runaway warning time was usually greater at lower C rates and lower temperatures (2C at 25ºC gave 1h warning, whereas 1C at 45ºC and 3C at 25ºC both gave 10 mins). Failure probability increased rapidly with cell temperature, reaching 83 – 90% immediately before failure.

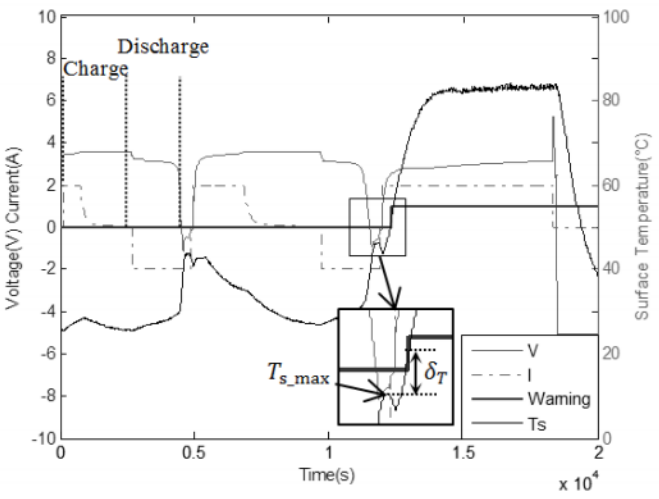

Fig. 4 – shows V, I, and cell surface temperature for a 2C discharge at 25°C ambient temperature. The region in which the temperature rule is satisfied is magnified [13].

The authors note that the technique should be applicable to most Li-ion chemistries, though do not specifically state which ones, and assert that testing needs to be carried out on a wider range of cells (only one model was tested in this study). An interest in future application of this technique to larger battery packs is expressed by the group.

The same technique was explained in a patent application by Xie (2013), which explains how such measurements may be performed by a standalone measurement and processing device, and it is noted in the same document that rapid increases in contact resistance and SEI resistance could be used to predict TR multiple cycles before such an event may happen [14]. The system therefore also includes hardware for impedance monitoring and analysis, but it is not made clear how this system functions, or as to whether the system has been successfully utilised.

It is clear that this technique must be studied in greater depth using a wider range of cell chemistries, pack complexities, and cell geometries to determine the extent of its value.

The EU Stallion Project (2015), has found that acoustic emissions and mechanical strain may provide an early warning of TR [15]. During operation Li ion cells produce acoustic emissions that can be detected using a surface sensor, and mechanical strains that result from gas evolution and Li insertion – these can be detected using a strain gauge.

By using both sensing methods, it was possible to predict TR in overcharged cells before onset; acoustic emission rates were seen to increase before onset of TR, and strain was seen to increase rapidly before failure (although it is noted a large temperature variation way cause the measurement reliability of a strain gauge to decrease.

3.3 Screening for Elevated Self-Discharge to Detect Shorts in Real World Systems

TIAX (2014) filed patent for a system with the capability to detect internal shorting via the monitoring of self-discharge rate (fig. 5) [16]. A simple version of the system was tested on cells containing a series of deliberate internal shorts, and the accuracy and reliability of the monitoring system was confirmed [17]. The patent explains the theory and operation of the system, and makes suggestions for alternative operating modes and sensor configurations.

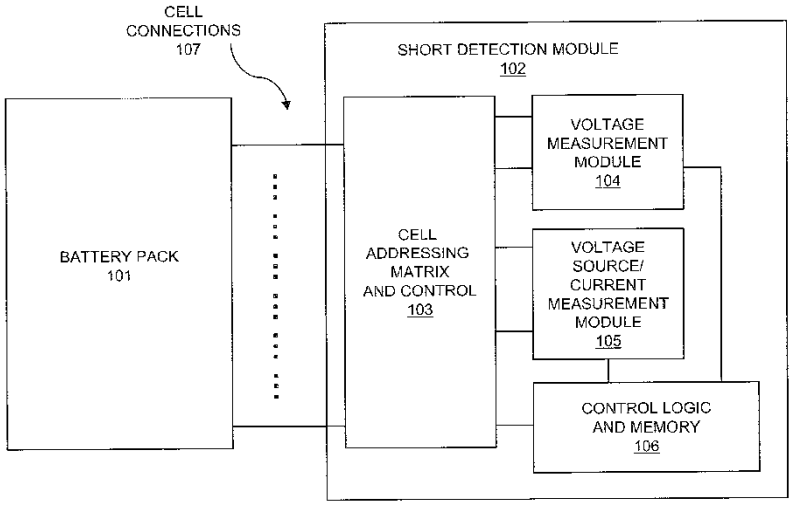

Fig. 5 – A schematic representation of the components that make up the TIAX short detection module.

The testing process is as follows: The short detection module makes connection with the battery pack and determines whether it is at rest. Once it has been confirmed that the pack is at rest, it is allowed a further rest period, the duration of which is based on cell chemistry and properties. A cell or block of cells is then selected by the cell addressing and control module, and a voltage measurement is taken by the voltage measurement module, then recorded by the control logic and memory module.

The voltage source/current measurement module is set to output the voltage measured and recorded by the voltage measurement module, and the current flowing between the voltage source and the cell is measured (fig. 6). If a cell draws a non-zero, increasing current from the voltage source, a signal is sent to the control logic and memory component which raises a warning that is observable to the user. The testing process is repeated for each cell/block of cells connected to the short detection module.

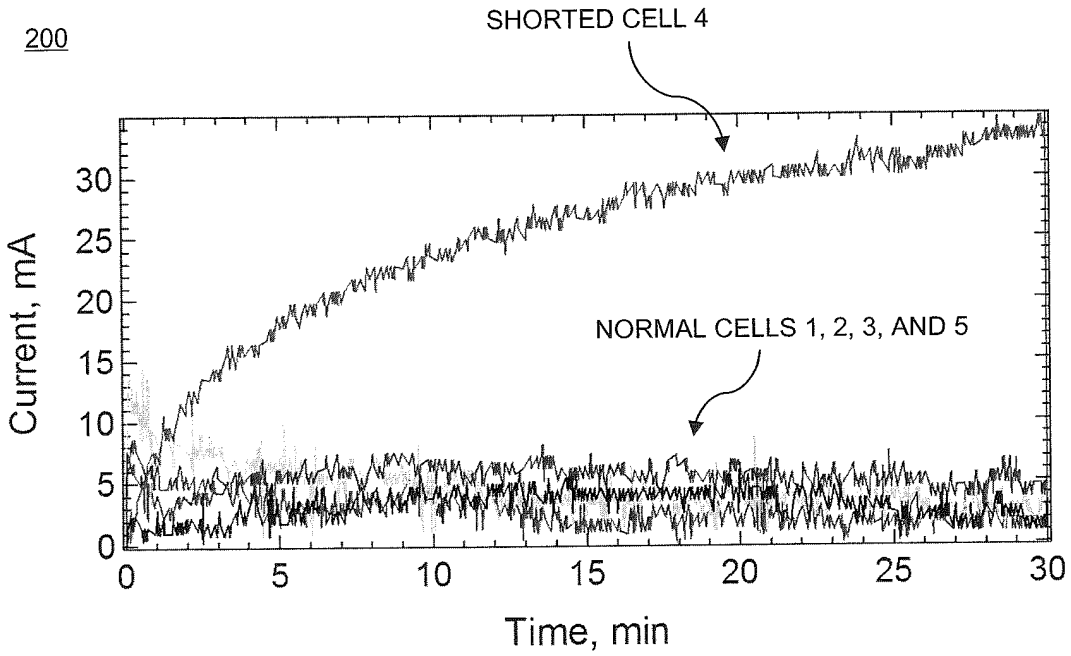

Fig. 6 – Shows the typical current draw for normal and shorted cells during the monitoring process [16].

It is noted that an abridged test, in which the voltage measurement module component is not used, can be performed. The cell or block of cells to be tested is connected immediately to the voltage source/current measurement module component, and voltage is varied until a near-zero current flow between the voltage source and cell is achieved. If the current flow is seen to increase over the course of a test, it is concluded that the cell contains an internal short.

The voltage source/current measurement module contains regulators that allow any cell voltage to be registered, maintained, and varied. This has been achieved using linear regulators, DC-DC converters, and inverting converters. It is noted that the output voltage of some regulators can be controlled via an input voltage, which may be delivered by a separate circuit.

Numerous current measurement methods are suggested, such as a resistor placed in the path between the voltage source and the battery (where current can be determined using ohms law) – the voltage signal is amplified to allow for a much smaller resistance value to be used (this reduces the effect of the resistor on the current signal). The utilization of Hall Effect transducers and flux gate (induction) transducers is also mentioned as a method of current measurement.

It is noted by the authors that the methods described were successful in detecting a 100 Ω short that had be manually inserted into one cell of a battery pack, and that the current monitoring test took 30 minutes to complete.

It is noted that if cells are to be tested in series blocks, a voltage source that can accurately reproduce multiples of the cell voltage must be integrated into the short detection module. It is also stressed that an increase in the number of individual cells or blocks to be tested simultaneously will increase the complexity of the hardware in the short detection module, but that this will be vital to ensure testing times do not become unreasonable (30 minutes per cell could increase to 40 h for an 80 cell EV pack).

A possible solution to long testing times is suggested in a 3rd test method. In this process, the voltage of the cell is measured, the same voltage is briefly applied to the cell by the voltage measurement and current measurement module, and then the source is disconnected for a predetermined period of time based on cell properties. After this, the voltage source is reconnected, and a short is identified by a surge in current (indicating that the cell has undergone significant self-discharge). During the disconnection period, the voltages across the other cells can be monitored, eliminating the need for multiple connections. It is mentioned that this method would greatly increase the complexity of the control, logic and memory component, and would probably require the development of an integrated circuit chip. It is also noted that the overall accuracy of the programmable input to the voltage source would need to be high. If a significant current flow is detected by the system (i.e. batteries are charging or discharging) the short testing will be immediately postponed.

It is suggested that the short detection module components may be integrated into a standalone unit which may be directly connected to a battery pack (i.e. the standalone unit will contain all wiring necessary), but that it may not be necessary to include voltage sensing components, as they are a general requirement of commercial Li-ion packs.

Considering that TIAX have successfully developed a system capable of screening for one of the behaviors observed in shorting cells, it does not seem unreasonable to suggest that it may be possible to develop systems that screen for fluctuating current and voltage, extended taper current, and unexpected changes in voltage, temperature, and resistance.

3.4 The Effect of Thermal Abuse on Measurable Cell Parameters

Feng (2014), performed differential scanning calorimetry experiments on 25 A h NCM prismatic packs composed of two pouch cells and an outer shell, with the aim of examining the effects of thermal abuse on voltage, resistance, and temperature differentials between various points within and outside the shell [18]. 4 thermocouples were connected to various points on the NCM pack (fig. 7), and the temperature

of the heater was gradually increased. Resistance monitoring was performed by administering 10 s constant voltage pulses to the cell, and dividing the applied voltage by the resulting current. The temperature detected by each thermocouple, the battery voltage, and the battery resistance were recorded at regular intervals.

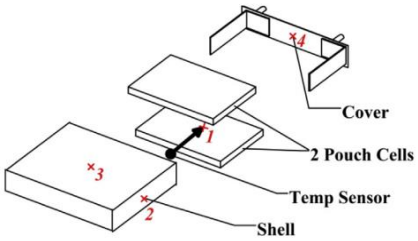

Fig. 7 – Shows the positions of thermocouples 1,2,3 and 4 in the cell casing.

The authors note 6 distinct sections of interest in the $\frac{dT}{dt}$ vs. T plot:

I. Capacity fade, no detectable self-heating
II. SEI decomposition, onset of detectable self-heating
III. Decrease in $\frac{dT}{dt}$ due to separator melting
IV. Acceleration in $\frac{dT}{dt}$ due to formation of microshorts and cathode decomposition.
V. $\frac{dT}{dt} > 1$ due to significant short circuits and exothermic processes. Thermal runaway occurs.
VI. EV-ARC temp warning triggers and system is cooled.

Results showed that the maximum difference between internal and external cell temperature reached 1°C roughly 6000 s before the cell entered TR, and at this point the temperature difference began to rise rapidly. This phenomena is not explored further by the author.

A sharp voltage drop was observed in all 4 experiments between 15-41 s before TR. It is noted that this phenomena may be a useful early warning signal for TR, though it does not satisfy the requirements of this literature review. The authors also note a gradual increase in cell resistance from 20 mΩ to 60 mΩ before TR (attributed to the separator shutdown process and further cell decomposition processes), then a sharp increase from 60 mΩ to 370 mΩ during the rapid temperature increase before failure (fig. 8)

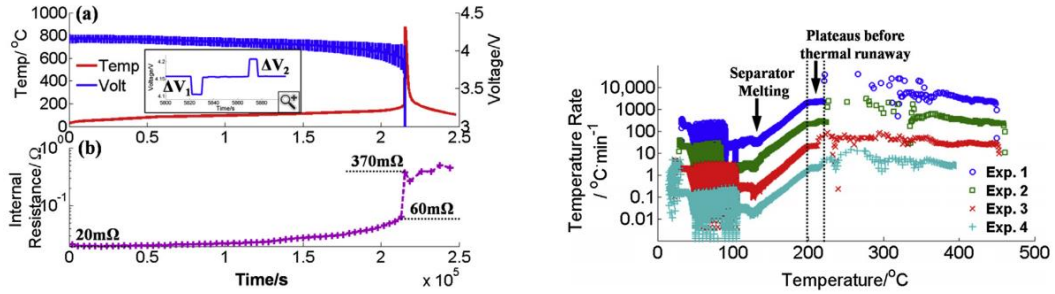

Fig. 8 – left (a), voltage and temperature as a function of time. Left (b), cell resistance as a function of time. Right, shows $\frac{dT}{dt}$ *vs. T – a decrease in* $\frac{dT}{dt}$ *can be seen at the separator melting temperature.*

It is not truly clear as to whether this increase in resistance is related to cell decomposition, a direct effect of elevated temperature, or a combination of both, but in any instance the rise in resistance may be used as an indicator of a rising cell temperature that could ultimately lead to cell runaway. Furthermore the clear changes in in $\frac{dR}{dt}$ that begin occurring at around $1.3x10^5$ s may be an easy to detect and reliable TR warning signal. The notable decrease in $\frac{dT}{dt}$ at the point of separator melting is recognised by the authors, and has been noted in other studies (fig. 9) [19]. Considering that this melting process is very likely to occur prior to venting and combustion, detection of the $\frac{dT}{dt}$ change could provide some degree of warning of TR.

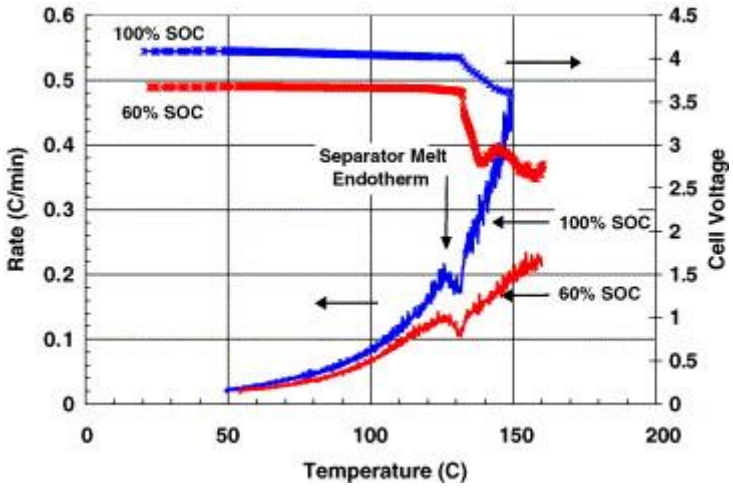

Fig. 9 – shows the change in heat evolution rate upon melting of the separator. This causes a decrease in $\frac{dT}{dt}$ *[19].*

It is worth noting that cell temperature will increase during charging, and cell resistance will change according to state of charge. It would therefore be important to understand and decouple these effects from any temperature and resistance monitoring processes to accurately determine whether a cell was progressing towards TR. Temperature differentials may be difficult to measure accurately for larger

packs using the method presented in this paper; an impractical number of thermocouples may be required for accurate and meaningful data to be obtained.

An important issue to consider is that thermal abuse is unlikely to occur over a long time period at a constant ramp rate in real-world scenarios; it is more likely that a cell may fail, resulting in combustion of vented gases that heat adjacent cells and induce runaway within minutes, or that a cell would be subjected to localised heating at a resistive joint. The experiments performed during this study were around 66 h in duration, and so temperature, resistance, and voltage profiles, and the timescale on which TR warning signs manifest may not be representative of real life applications.

4. Discussion

Research performed by Wu (2014), presents a potentially scalable technique that could be used to detect lithium dendrite formation long before it leads to cell shorting and joule heating. Application of this technique to commercial cells may allow for the detection of shorts that develop as a result of mechanical abuse, accidental overcharge, accidental over-discharge, overcurrent, contamination, and manufacturing faults, but may not be effective in situations of thermal abuse. Clearly, studies into the range of compatible cell chemistries and cell shapes must be performed, as investigations into the potential for scale-up are required.

Studies by Feng *et al.* (2014), show some interesting changes to easily measurable cell parameters that may occur during thermal abuse and TR. Due to the very controlled conditions under which thermal abuse was administered (very slow, constant ramp rate) it is not sensible to assume that the same response to thermal abuse would be observed in a field situation, however the failure signatures observed are significant enough to warrant further study. Although the voltage drop may provide a short warning (15-41 s) that should be sufficient to allow staff to retreat to safety, it is too short to be considered significant within the scope of this study. Changes in $\frac{dR}{dt}$, $\frac{dT}{dt}$, and R during separator shutdown may also be measurable, and if so could provide a much earlier warning of TR. The study performed by Xiong (2012) shows how logic may be applied to make use of the temperature and voltage signals as TR early warning signs in a cycling cell. Considering that most battery management systems already include voltage monitoring, and that temperature is measured from the battery surface (i.e. non-invasive) it seems possible that such a monitoring system could be integrated into larger pack systems.

The cycling tests performed by Mikolajczac *et al.* (2010), showed a range of behaviours that may indicate the presence of internal shorts, and it is interesting that TIAX (2014) were able to successfully detect internal shorts by screening for one of these behaviours (elevated self-discharge rate), and patent an entire short detection system for use on battery packs. It may therefore be possible to integrate other short screening processes into this system e.g. using similar logic processes to those developed by Xiong

(2012) we may be able to detect voltage and current fluctuations during charging, extended taper current times, or significant changes in discharge capacity between cycles.

A noteworthy observation is the narrow range of input parameter variation during the studies: temperatures are held within a narrow range of values during the Mikolajczac et al (2010) and Xiong (2012) studies, and state of charge is held almost constant during the study performed by Feng et al (2014). It is not possible, for example, to confidently predict the likelihood of a TR event occurring in a charging system based entirely on an abnormal $\frac{dT}{dt}$ if we do not fully understand how charging will effect T and are therefore unable to decouple T changes associated with charging and T changes associated with separator melting. Similarly, the Xiong (2012) study shows changes in the proximity of the warning signals to the TR event at a narrow range of different C-rates and ambient temperatures, but does not provide enough data for these relationships to be fully understood. The study also highlights the need to determine separate voltage and temperature threshold parameters for multiple different cell chemistries and shapes. To build a fully reliable early warning system this complex relationship between cell parameters must be understood to the extent that it becomes somewhat predictable.

5. Conclusion

Although the range of literature related to this topic is extremely limited, it has been demonstrated that easy to measure signals can provide us with information relating to the internal environment of a Li-ion cell, and it may be possible to monitor and analyse these signals in a variety of ways that could allow us to accurately predict both the likelihood and proximity of a TR event. Furthermore it has been shown that a minor redesign of the cell separator can provide us with a warning of impending internal short formation long before such a short fully develops (although the logistical problems associated with this modification may affect the prospects of implementing it).

The significant challenges relating to cell chemistry compatibility, cell shape compatibility, scale-up, and the relationship between cell parameters would all need to be resolved before TR early warning technology could possibly be implemented, though based on the information reviewed development of a reliable early warning system should not yet be ruled out as an impossible task.

6. References

[1] P. Miller, Automotive Lithium-Ion Batteries (2015) *Johnson Matthey Technol. Rev.*, 59 (1), pp. 4 - 12.

[2] A. Vayryman, J. Salminen (2012) Li Ion Battery Production, *J. Chem. Thermodynamics*, 46 (1), pp. 80-85.

[3] Q. Wan, P. Ping, X. Zhao, G. Chu, J. Sun, C. Chen (2012) Thermal runaway caused fire and explosion of lithium ion battery, *J. Power Sources*, 208, pp. 210-224.

[4] NTSB (2013), Auxiliary Power Unit Battery Fire, pp. 30 – 66.

[5] Q.S. Wang, J.H. Sun, G.Q. Chu (2005) Fire Safety Science – Proceedings of the Eighth International Symposium International Association for Fire Safety Science, Beijing, pp. 375–382.

[6] D. Lisbona, T. Snee (2011) A review of hazards associated with primary lithium and lithium-ion batteries, *Process Safety and Environmental Protection*, 89, pp. 434 - 442.

[7] The Fire Protection Research Foundation (2011) Lithium-Ion Batteries Hazard and Use Assessment, pp. 30 – 81.

[8] C. Mikolajczak (2011) *Lithium-Ion Batteries Hazard and Use Assessment*, Press: Springer US, New York.

[9] D.Fouchard, L. Lechner (1993) Analysis of safety and reliability in secondary lithium batteries, *Electrochimica Acta*, 38 (9), pp. 1193 – 1198.

[10] E. Darcy, M. Keyser (2014) On-Demand Cell Internal Short Circuit Device – Proceedings of the Power Sources Conference, Orlando, pp. 1 – 4.

[11] H. Wu, D. Zhuo, D. Kongg, Y. Cui (2014) Improving battery safety by early detection of internal shorting with a bifunctional separator, *Nature Communications*, 5, pp. 1-6.

[12] C. Mikolajczak, J. Harmon, K. White, Q. Horn, M. Wu, K. Shah (2010) Detecting lithium-ion cell internal fault development in real time, *Power Electronics Technology*.

[13] J. Xiong, H. Banvait, L. Li (2012) Failure Detection of Over-Discharged Li-ion Batteries – Proceedings of the Electric Vehicle Conference, Greenville, SC, pp. 1 – 5.

[14] J. Xie, J. Chen, L. Li, Y. Chen (2013) Advanced battery early warning and monitoring system, US Patent: US 20130135110 A1.

[15] G. Mulder (2015) Safety of large stationary Li-ion systems - Proceedings of the International Renewable Energy Storage conference, Dusseldorf, pp 33 - 40.

[16] TIAX (2014) System and methods for detection of internal shorts in batteries, US Patent: US 20140266229 A1.

[17] TIAX [2013] Lithium-Ion Battery Safety: Detection of Developing Internal Shorts and Suppression of Thermal Runaway, pp. 1 – 4.

[18] X. Feng, M. Fang, X. He (2014) Thermal runaway features of large format prismatic lithium ion battery using extended volume accelerating rate calorimetry, *J. Power Sources*, 255, pp. 294 – 301.

[19] E. P. Roth, D. H. Doughty (2004), Thermal abuse performance of high-power 18650 Li-ion cells, *J. Power Sources*, 128 (2), pp. 308-318.